



# MicroRNA-133b Inhibits Tumor Cell Proliferation, Migration and Invasion by Targeting SUMO1 in Endometrial Carcinoma

Technology in Cancer Research & Treatment  
 Volume 20: 1-12  
 © The Author(s) 2021  
 Article reuse guidelines:  
[sagepub.com/journals-permissions](http://sagepub.com/journals-permissions)  
 DOI: 10.1177/15330338211065241  
[journals.sagepub.com/home/tct](http://journals.sagepub.com/home/tct)  


Lingyun Liao<sup>1,#</sup>, Yun Chen<sup>1,#</sup>, Jieli Zhou<sup>1</sup>, and Jing Ye<sup>2</sup> 

## Abstract

**Objectives:** An increasing number of studies have confirmed that microRNAs (miRNAs/miRs), as oncogenes or tumor suppressor genes, play an important regulatory role in the occurrence and development of numerous types of cancer. The aim of the present study was to investigate the potential role and mechanism of *miR-133b* and small ubiquitin like modifier 1 (SUMO1) in the development of endometrial carcinoma (EC). **Methods:** First, Venn diagrams are used to identify the differential expressions of miRNAs in EC from GSE35794 and GSE25405 datasets. Next, we conduct a series of functional tests, including Cell Counting Kit-8, wound healing, and transwell and matrigel assays. Then, a bioinformatics tool, is used to identify downstream target genes of *miR-133b* and to verify the predicted results by RT-qPCR, Western blotting and double luciferase reporter gene analysis. Finally, in order to further study whether the cellular function of *miR-133b* is mediated by the expression of *SUMO1*, rescue experiments were carried out. **Results:** The results of bioinformatics studies showed that the expression of *miR-133b* was down-regulated in EC tissues, and the expression level of *miR-133b* was lower in patients with high grade, different histology or menopausal status. The results of functional assay showed that overexpression of *miR-133b* reduced cell proliferation, migration and invasion. On the contrary, *miR-133b* silence has the opposite effect. *SUMO1* was the direct target of *miR-133b* and was negatively regulated by *miR-133b*. The decrease of *SUMO1* mRNA expression inhibited the proliferation, migration and invasion of EC cells, and reversed the effect of *miR-133b* on EC cells. **Conclusion:** The findings from the present study suggested that *miR-133b* may be a tumor suppressor gene and a potential therapeutic target for the treatment of EC.

## Keywords

endometrial carcinoma, *miR-133b*, *SUMO1*, proliferation, migration, invasion

## Abbreviation

EC, endometrial carcinoma; miRNAs/miRs, microRNAs; *SUMO1*, small ubiquitin like modifier 1; GEO, Gene Expression Omnibus; OS, overall survival; RFS, relapse-free survival; NC, negative control; CCK-8, Cell Counting Kit-8; RT-qPCR, RNA extraction and reverse transcription-quantitative PCR; WT, wild-type; MUT, mutant-type; SD, standard deviation; PPI, protein-protein interaction; STRING, Search Tool for the Retrieval of Interacting Genes/Proteins

Received: April 14, 2021; Revised: October 22, 2021; Accepted: November 12, 2021.

## Introduction

Endometrial carcinoma (EC) is one of the most common malignant tumors in the female reproductive system.<sup>1</sup> In recent years, the incidence and mortality rates of EC have been increasing due to the changes in lifestyle. EC is divided into type I (estrogen-dependent) and type II (estrogen independent) according to the clinical and endocrine characteristics. Type I EC accounts for ~85% of all cases.<sup>2</sup> At present, the treatment of EC primarily involves surgery, radiotherapy, chemotherapy, hormone therapy and new targeted therapy, as adjuvant

<sup>1</sup> First Affiliated Hospital of Gannan Medical University, Ganzhou, China

<sup>2</sup> School of Clinical Medicine, Jiangxi University of Traditional Chinese Medicine, Nanchang, China

# Lingyun Liao, Yun Chen Joint first authors

### Corresponding Author:

Jing Ye, School of Clinical Medicine, Jiangxi University of Traditional Chinese Medicine, No. 1688 Meiling Avenue, Xinjian District, Nanchang, Jiangxi 330004, China.

Email: yejing0519@163.com



therapeutic approaches for EC.<sup>3</sup> However, the 5-year survival rate for patients with EC has not significantly improved. Therefore, further understanding into the molecular mechanism of EC would enable the identification of novel therapeutics for the prevention, diagnosis and treatment of EC.

MicroRNAs (miRNAs/miRs) are a type of endogenous small RNA and are 18 to 24 nucleotides in length. miRNA is an important regulatory factor, which plays a key role in various cellular processes and biological activities, including cell proliferation, migration, metastasis, apoptosis, autophagy and invasion.<sup>4-7</sup> miRNAs regulate gene expression by targeting the 3'-untranslated region (UTR) of mRNA, inhibiting or directly degrading target mRNA at the translational level. Previous studies have revealed that the abnormal expression of miRNAs in malignant tumor cells plays a crucial role in the multi-step process of carcinogenesis, from initiation and development, to the acquisition of metastatic features.<sup>8-10</sup> In recent years, an increasing number of studies have shown that the differential expression of miRNAs has been associated with the occurrence and development of EC, and the functional role and mechanism of miRNAs in EC have been widely investigated. For example, *miR-486 to 5p* was demonstrated to promote cell proliferation, migration and invasion by targeting *MATK1* in EC.<sup>11</sup> In addition, *EIF4E*-related *miR-320a* and *miR-340 to 5p* inhibited the metastasis of EC cells by preventing *TGF-β1*-induced epithelial-mesenchymal transition.<sup>12</sup> Upregulation of *miR-103* also promoted the progression of EC by targeting *ZO-1*.<sup>13</sup> However, to the best of our knowledge, the function of *miR-133b* in EC has never been reported. Several studies have indicated that *miR-133b* could function as a tumor suppressor in various types of cancer. For example, *miR-133b*, derived from exosomes, was downregulated in bladder cancer cells, and overexpression of *miR-133b* inhibited bladder cancer proliferation by upregulating *DUSP1*.<sup>14</sup> In addition, overexpression of *miR-133b* inhibited the phosphorylation of *ERK1/2* and reduced the activity of the *ERK* signaling pathway thus, inhibiting the proliferation, migration and invasion of renal cell carcinoma cells and improving their chemosensitivity.<sup>15</sup> Similarly, the mRNA expression level of *miR-133b* was downregulated in non-small cell lung cancer and was associated with lymph node metastasis.<sup>16</sup> Studies have shown that small ubiquitin like modifier 1 (*SUMO1*) functions as ubiquitin, which binds to the target protein, as part of the post-translational modification system.<sup>17</sup> *SUMO1* has been considered to play a critical role in the occurrence and development of different types of malignancies, and the expression level of *SUMO1* in malignant tumors was significantly increased.<sup>18</sup> In addition, *SUMO1* modification of *Mettl3* promoted tumor progression by regulating Snail mRNA homeostasis in hepatocellular carcinoma<sup>19</sup> and the protein, sumoylation, with *SUMO1* promoted by Pin1 in glioma stem cells, increased the malignancy of glioblastoma.<sup>20</sup> Therefore, we hypothesize that *miR-133b* may play a role as a tumor suppressor gene in EC by regulating *SUMO1*.

In the present study, the mRNA expression level of *miR-133b* was detected in EC cell lines, include Ishikawa, HEC-1A, HEC-1B, RL95 to 2. and the functional roles of *miR-133b* in the regulation of proliferation, migration and

invasion of EC cells was also investigated, as well as determining the potential mechanism of *miR-133b*.

## Materials and Methods

### Bioinformatics Analysis

The miRNA expression datasets related to EC were downloaded from the Gene Expression Omnibus database (GEO, <https://www.ncbi.nlm.nih.gov/geo/>, Created in 2000)<sup>21</sup> to identify differentially expressed miRNAs. Using  $|\log_2 \text{fold change}| > 1$  and  $p < 0.05$ , as filtering criteria, the differentially expressed miRNAs from the GSE35794 and GSE25405 datasets were identified using GEO2R. A volcano map was constructed using the SangerBox platform to visualize the differentially expressed miRNAs. In addition, the intersection of up- and downregulated miRNAs in the GSE35794 and GSE25405 datasets were obtained using a Venn diagram (<https://bioinfogp.cnb.csic.es/tools/venny/>).<sup>22</sup> The mRNA expression level of *miR-133b* in EC based on tumor grade, histology and menopause status were analyzed using the UALCAN database. In addition, the PirTar, miRanda, TargetsCan and miRDB databases were used to predict the target genes of *miR-133b*, following which, the Kaplan-Meier Plotter database (<http://kmplot.com/analysis/>, Created in 2009)<sup>23</sup> was performed to obtain the survival curves of overall survival (OS) and relapse-free survival (RFS) times with respect to expression level of *SUMO1*. Furthermore, Search Tool for the Retrieval of Interacting Genes/Proteins (STRING; <https://string-db.org/>)<sup>24</sup> and Cytoscape were used to identify potential target genes.

### Cell Culture and Transfection

The RL95 to 2 (No.TCHu198), Ishikawa, HEC-1-A(No.TCHu149) and HEC-1-B(No.TCHu115) EC cell lines were purchased from Shanghai Chinese Academy of Sciences Cell Bank and were cultured in DMEM, containing 10% FBS (Gibco; Thermo Fisher Scientific, Inc.; Cat: 10099141C) and 1% penicillin/streptomycin (Gibco; Thermo Fisher Scientific, Inc.; Cat: 15140148) at 37 °C in a humidified incubator with 5% CO<sub>2</sub>. The RL95 to 2 and HEC-1-A cell lines were transfected with negative control (NC) mimic, *miR-133b* mimic, NC inhibitor or *miR-133b* inhibitor (all cell lines were purchased from Guangzhou RiboBio Co., Ltd). Lipofectamine® 2000 (Invitrogen; Thermo Fisher Scientific, Inc.; Cat: 11668019), was used for transfection, according to the manufacturer's instructions and subsequent experimentation was performed 48 h following.

### Cell Counting Kit-8 (CCK-8) Assay

The EC cell lines were seeded in 96-well plates, at a density of  $5 \times 10^3$  per well, then transfected with *miR-133b* mimics, *miR-133b* inhibitors, si-SUMO1 or their respective NCs. A total of 10 μl CCK-8 solution was added to each well, after the cells were cultured for 24, 48 and 72 h. After incubation at 37 °C for 2 h, the absorbance was detected at 450 nm using a Multiskan MS microplate reader (Thermo Fisher Scientific, Inc.).

### Transwell and Matrigel Assays

Transwell and massays were used to perform cell vertical migration and invasion analyses. The RL95 to 2 cell line were transfected with NC inhibitor or *miR-133b* inhibitor, and the HEC-1-A cell line were transfected with NC mimic or *miR-133b* mimic, for 48 h. Following which, the cells were made into a suspension using serum-free medium and added to the upper chamber, and medium containing 20% FBS was added into the bottom chamber. The cells were fixed with 4% paraformaldehyde for 15 min, then stained with 0.1% crystal violet for 20 min, 48 h later. The matrigel assay was performed using the same method, except that matrigel-coated membranes were used. The number of migrated or invaded RL95 to 2 and HEC-1-A cells were captured using a light microscope (Olympus Corporation).

### Wound Healing Assay

The RL95 to 2 and HEC-1-A cell lines were seeded in 6-well plates and cultured to ~80% confluence. After the plasmid was transfected with NC mimic, *miR-133b* mimic, NC inhibitor or *miR-133b* inhibitor, the monolayer was scratched using a 10  $\mu$ l pipette tip to create the wound, then it was gently washed with PBS to remove the floating cells. The wound width at 0, 24, 48 and 72 h was measured under a microscope (Olympus Corporation).

### RNA Extraction and Reverse Transcription-Quantitative PCR (RT-qPCR) Assay

Total RNA (20 mg) was extracted from the RL95 to 2 and HEC-1-A cell lines using TRIzol® (Invitrogen; Thermo Fisher Scientific, Inc.) according to the manufacturer's protocol. The quantitative real-time polymerase chain reaction (qRT-PCR) was performed on a NanoDrop One system (Merinton Instrument, Ltd) according to the manufacturer's instructions. To detect the expression levels of mRNA, first-strand cDNA was generated using the UEIris RT-PCR System for First-Strand cDNA Synthesis (Suzhou Purification Engineering Installation Co., Ltd, Suzhou, China) and RT-qPCR was conducted using the 2X SYBR Green qPCR Master Mix (Suzhou Purification Engineering Installation Co., Ltd, Suzhou, China). The mRNA expression levels of *SUMO1* was normalized to that of the housekeeping gene, glyceraldehyde-3-phosphate dehydrogenase (GAPDH). To detect the expression levels of miRNA, the first strand cDNA (tailing method) was used, according to the manufacturer's instructions. U6 was used as the endogenous control for *miR-133b*. The following thermocycling conditions were used: Initial denaturation at 95 °C for 5 min, followed by 35 cycles at 95 °C for 15 sec, 58 °C for 25 sec, and 72 °C for 25 sec, and final extension at 72 °C for 5 min. The relative mRNA expression levels was calculated using the  $2^{-\Delta\Delta Cq}$  method. The primer sequences (primer premier 5) are shown in Table 1.

**Table 1.** List of primers used in this study.

Primer	Sequence
miR-133b	5'-UUUGGUCCCCUUAACCAGCUA-3'
Universal primer	5'-GCGAGCACAGAATTAATACGAC-3'
U6	Forward: 5'-CTCGCTTCGGCAGCAC-3' Reverse: 5'-AACGCTTCACGAATTTGCGT-3'
GAPDH	Forward: 5'-ACGGATTGGTCGTATTGGGCG-3' Reverse : 5'-GCTCCTGGAAGATGGTGATGGG-3'
SUMO1	Forward: 5'-CGAGGCGTAGCGGAAGTTAC-3' Reverse : 5'-TCCTCCATTCCCAGTTCTTTTG-3'

### Western Blot Assay

The RL95 to 2 and HEC-1-A cell lines were harvested using a RIPA buffer, containing 1% protease inhibitors and the concentration of the total protein was measured using a BCA kit (Beyotime Institute of Biotechnology). The proteins were separated using a 12% SDS-PAGE and transferred to polyvinylidene fluoride (PVDF) membranes (EMD Millipore). Subsequently, the protein bands were blocked with 5% skimmed milk in TBS-Tween-20 buffer, then incubated with the following primary antibodies: *SUMO1* (cat. no. A19121) and GAPDH (cat. no. A19056) (both from ABclonal Biotech Co., Ltd) diluted at 1:1000. A goat anti-rabbit (cat. no. AS014) or a goat anti-mouse (cat. no. AS003) (both from ABclonal Biotech Co., Ltd) diluted at 1:10,000 was used as the secondary antibody. An enhanced chemiluminescence (EMD Millipore) substrate was used to visualize the bands, and the intensity of the bands was quantitatively analyzed using Image J (National Institutes of Health).

### Luciferase Reporter Assay

To validate the direct binding of *miR-133b* to the 3'UTR of *SUMO1*, wild-type (WT) or mutant-type (MUT) 3'UTR *SUMO1* were amplified and ligated into the psiCHECK-2 reporter plasmid to construct WT-*SUMO1* and MUT-*SUMO1* recombinant plasmids, respectively. The 293 T cells were seeded into 24-well plates and co-transfected with WT-*SUMO1* or MUT-*SUMO1* and *miR-133b* mimic, NC mimic, *miR-133b* inhibitor or NC inhibitor using Lipofectamine® 2000. Luciferase activity was measured after transfection for 48 h, using a luciferase assay system (Promega Corporation). The renin luciferase plasmid, pRL-TK was used as the positive control.

### Statistical Analysis

All the aforementioned experiments were conducted at least three times, and the data are presented as the mean  $\pm$  standard deviation (SD). All statistical analyses were performed using the GraphPad Prism V8 software (GraphPad Software Inc.).

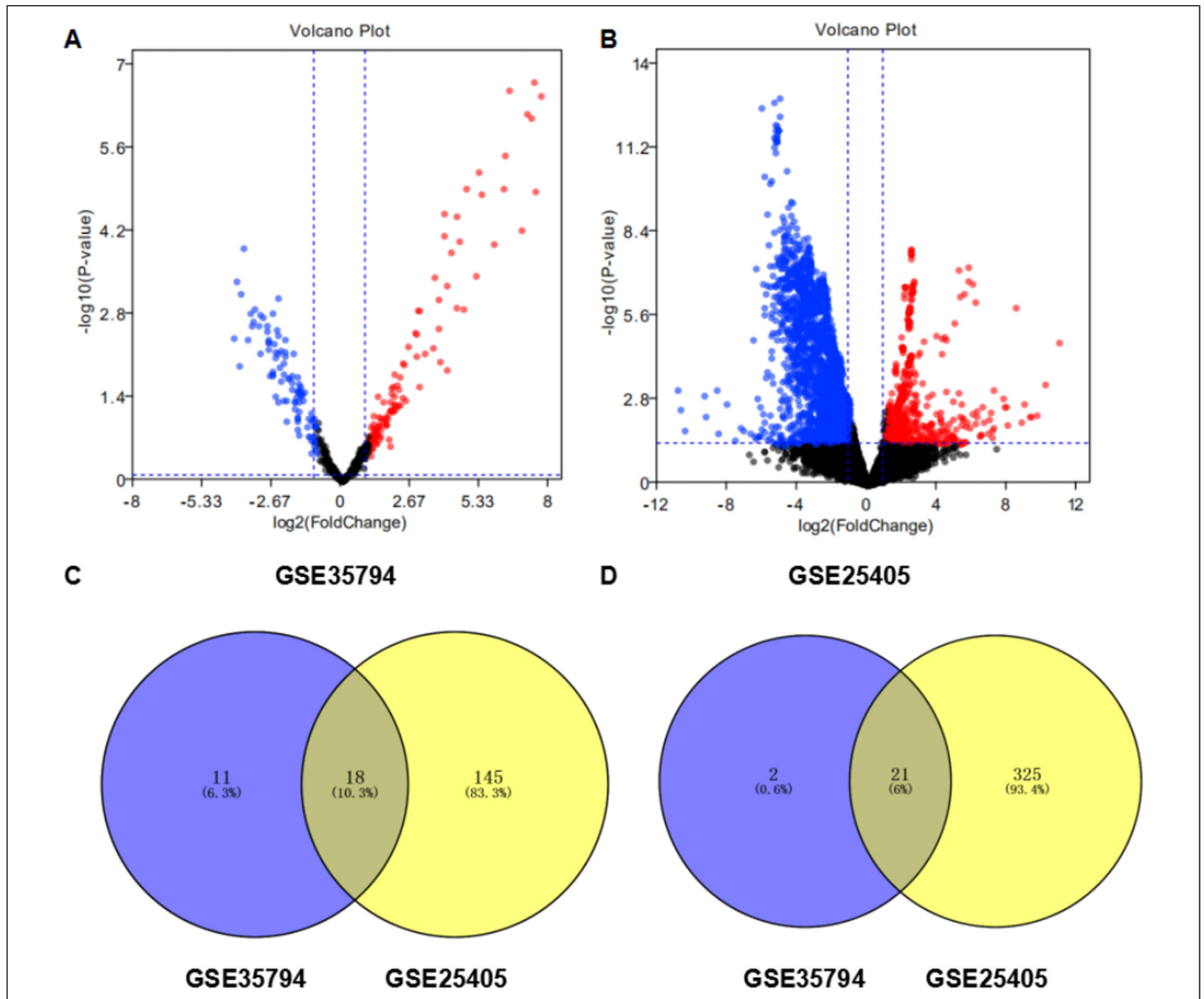


**Figure 1.** Volcano plots and venn diagrams. Volcano plots of the DEMs between endometrial carcinoma and adjacent tissues from the (A) GSE35794 and (B) GSE25405 datasets. The two datasets showed an overlap of (C) upregulated and (D) downregulated DEMs. DEMs, differentially expressed miRNAs.

A Student's t-test or an one-way ANOVA was used to investigate the significance of the difference between two groups or multiple groups, respectively. The post hoc test of one-way ANOVA was Sidak.  $p < 0.05$  was considered to indicate a statistically significant difference.

## Results

### Identifying Differentially Expressed miRNAs

The analysis of the GSE35794 and GSE25405 datasets was performed using the GEO2R online tool and the differential expression of the miRNAs was visualized using volcano plots. The red and green dots represent the miRNAs significantly up- or downregulated, respectively. Of these, 29 and

23 miRNAs were up- and downregulated in the GSE35794 dataset, while there was 143 and 346 miRNAs up- and downregulated in the GSE25405 dataset, respectively (Figure 1A and B). By crossing the two datasets, 18 up- and 21 downregulated miRNAs were identified (Figure 1C and D). Among them, the mRNA expression level of *miR-133b* was the lowest and *miR-200b* was the highest in EC. After reviewing previous studies, it was found that, to the best of our knowledge, *miR-133b* had never been reported in EC; therefore, *miR-133b* was selected for further analysis. Subsequently, the mRNA expression level of *miR-133b* in EC was investigated using the UALCAN database. As shown in Figure 2, *miR-133b* was notably downregulated in EC and patients with high grade tumors, different histology or menopause status expressed lower *miR-133b* expression levels. These

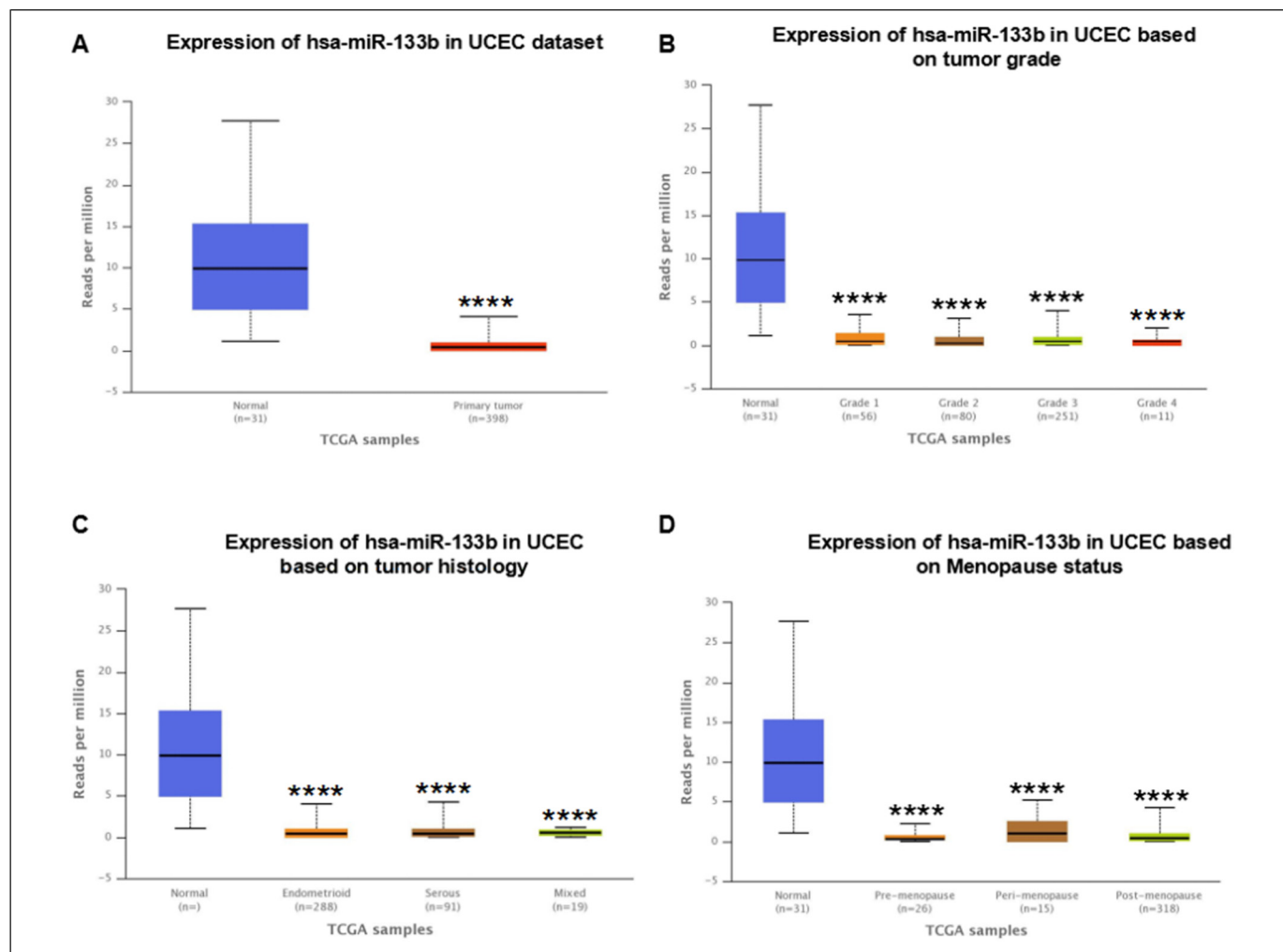


**Figure 2.** Expression level of *miR-133b* in EC. Expression level of *miR-133b* in EC. (A) and adjacent normal tissues, (B) based on tumor grade, (C) based on tumor histology and (D) based on menopause status. \*  $p < 0.05$ ; \*\*  $p < 0.01$ ; \*\*\*  $p < 0.001$ ; \*\*\*\*  $p < 0.0001$ .

results indicated that *miR-133b* was downregulated in EC and associated with tumor grade, different histology and menopause status.

### Expression Level and Transfection Efficiency of *miR-133b* in EC Cell Lines

The mRNA expression level of *miR-133b* in four EC cell lines (RL95-2, Ishikawa, HEC-1-A and HEC-1-B) was investigated and the RT-qPCR results indicated that the relative expression level of *miR-133b* was the highest in the RL95 to 2 cell line and lowest in the HEC-1-A cell line (Figure 3A;  $p < 0.0001$ ). Therefore, the HEC-1-A cell line was selected for *miR-133b* overexpression and the RL95 to 2 cell line was selected for *miR-133b* knockdown. Then, the expression efficiency of *miR-133b* after 48 h transfection was detected and the results showed that the mRNA expression level of *miR-133b* was elevated 13.88 times in the HEC-1-A cell line transfected with *miR-133b* mimic

(Figure 3B;  $p < 0.0001$ ), and decreased 0.47 times in the RL95 to 2 cell line transfected with *miR-133b* inhibitor (Figure 3C;  $P < 0.001$ ).

### *miR-133b* Inhibits EC Cell Proliferation, Migration and Invasion

A series of assays were used to elucidate the biological functions of *miR-133b* in the EC cell lines *in vitro*. As shown in Figure 4A, transfection with *miR-133b* mimic inhibited HEC-1-A cell proliferation at 48 ( $p < 0.0001$ ) and 72 h ( $p < 0.001$ ), while the *miR-133b* inhibitor exerted the opposite effect on the proliferation of the RL95 to 2 cells at 48 ( $p < 0.05$ ) and 72 h ( $p < 0.0001$ ). In addition, the effect of *miR-133b* on cell migration and invasion was determined. As shown in Figure 4B, a wound healing assay was used to detect the ability of cell migration, and it was found that the wound width of the HEC-1-A cell line transfected with *miR-133b* mimics was significantly decreased, 48 ( $p < 0.05$ ) and 72 h ( $p$

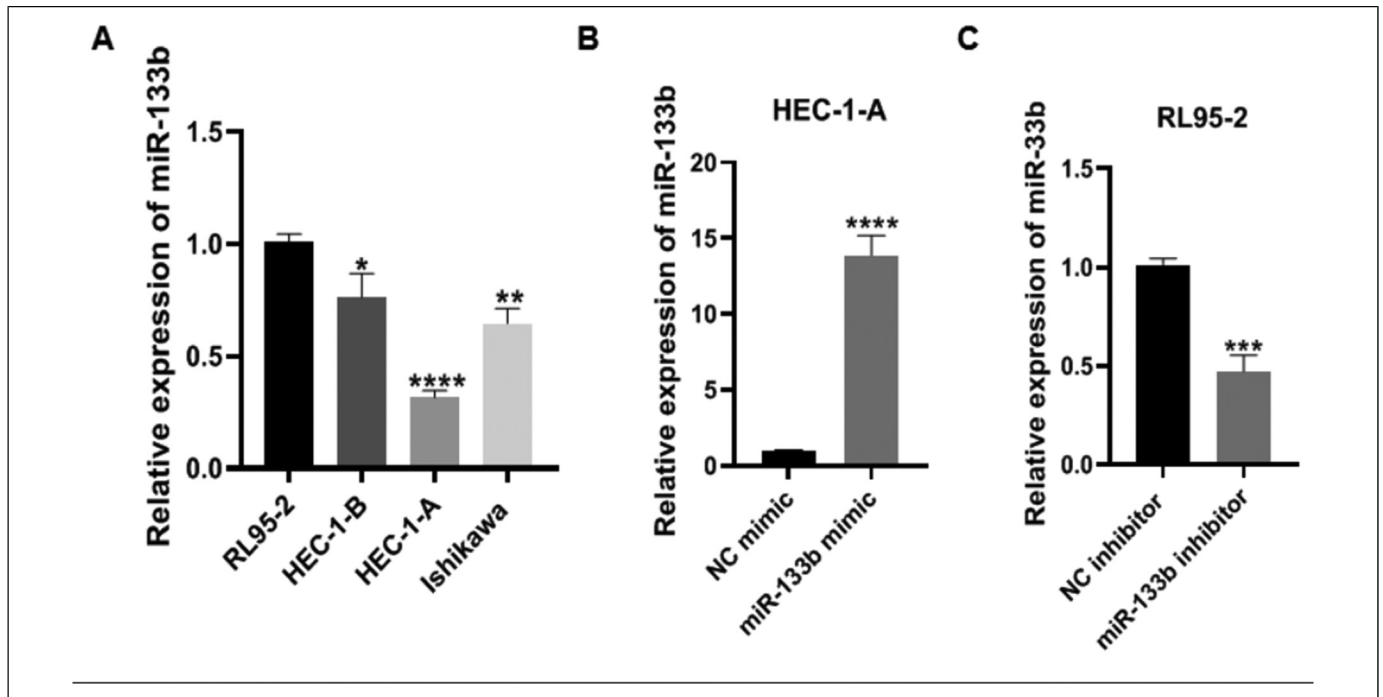


**Figure 3.** Expression and transfection efficiency of *miR-133b* in the endometrial carcinoma cell lines. (A) The mRNA expression level of *miR-133b* in the RL95 to 2, HEC-1-B, HEC-1-A and Ishikawa cell lines were detected using reverse transcription-quantitative PCR. The expression level of *miR-133b* in (B) the HEC-1-A cell line transfected with NC or *miR-133b* mimic and (C) the RL95 to 2 cell line transfected with NC or *miR-133b* inhibitor. \*  $p < 0.05$ ; \*\*  $p < 0.01$ ; \*\*\*  $p < 0.001$ ; \*\*\*\*  $p < 0.0001$ .

$< 0.01$ ), following transfection, while the *miR-133b* inhibitor had the opposite effect at 48 ( $p < 0.05$ ) and 72 h ( $p < 0.05$ ). Transfection with *miR-133b* mimic attenuated HEC-1-A cell invasion and migration (Figure 4C;  $p < 0.05$ ), while the *miR-133b* inhibitor had the opposite effect on RL95 to 2 cellular behavior (Figure 4C;  $p < 0.05$ ). Collectively, these results demonstrated that overexpression of *miR-133b* suppressed the proliferation, migration and invasion in the EC cell lines.

### *SUMO1* is a Target Gene of the *miR-133b*

The target genes of *miR-133b* were predicted using the miRanda, PirTar, Targetscan and miRDB online tools, which revealed 735, 405, 503 and 655 candidate genes, respectively. As shown in Figure 5A, the Venn diagram displayed the candidate genes from four mRNA-miRNA prediction databases, including 160 intersection genes. In addition, the 160 genes were imported into the STRING database to construct a protein-protein interaction network (Figure 5B), then the top 10 hub genes were screened using the cytoHubba plug-in, in Cytoscape (Figure 5C). Subsequently, the mRNA expression levels of the top three genes, *SUMO1*, *XPO1* and *SIRT1* were identified using the GEPIA database, and only *SUMO1* was found to be downregulated in EC (Figure 5D;  $p < 0.05$ ). Furthermore, the OS and RFS times in patients with EC and high *SUMO1* mRNA expression levels were poor (Figure 5E;  $p < 0.01$  and  $p < 0.05$ , respectively). The aforementioned results suggested that *SUMO1* may be the target gene of

*miR-133b* using bioinformatics analysis. Next, experimental verification was performed.

### *SUMO1* is a Direct Target Gene of *miR-133b* in EC Cells

To investigate whether *SUMO1* is the target gene of *miR-133b*, a luciferase reporter assay was used to detect the direct binding sites of *miR-133b* in its 3'UTR. As shown in Figure 6A, *miR-133b* mimic decreased luciferase activity in the *SUMO1* to 3'UTR-WT 293 T cells ( $p < 0.05$ ); however, there was no significant effect in the *SUMO1* to 3'UTR-MUT 293 T cells compared with that in the NC mimic group. In addition, the *miR-133b* inhibitor notably increased luciferase activity in *SUMO1* to 3'UTR-WT 293 T cells ( $p < 0.05$ ), while there was no effect in the *SUMO1* to 3'UTR-MUT 293 T cells. To further characterize the association between *miR-133b* and *SUMO1*, the mRNA and protein expression levels of *SUMO1*, following overexpression and knockdown of *miR-133b* in both the HEC-1-A and RL95 to 2 cell lines was investigated. It was observed that the mRNA expression level of *SUMO1* was increased in the RL95 to 2 cells transfected with *miR-133b* inhibitor, while decreased expression levels were found in the HEC-1-A cell line following transfection with *miR-133b* mimic (Figure 6B; both  $p < 0.01$ ). The same trend was also found in the protein expression level of *SUMO1* (Figure 6C;  $p < 0.001$  and  $p < 0.01$ , respectively). Taken together, the results suggested that *miR-133b* targeted *SUMO1* and negatively regulated its expression.



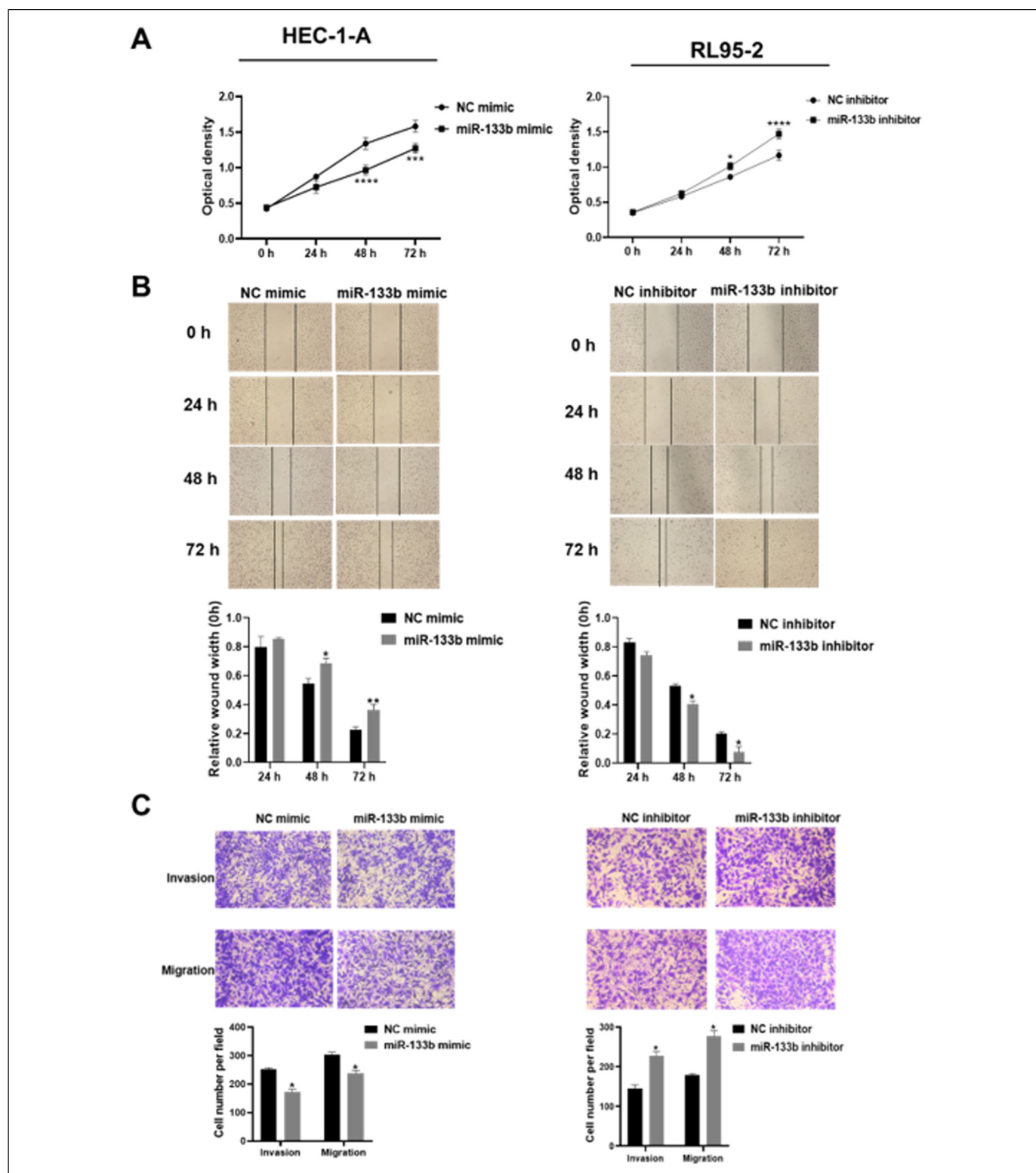


**Figure 4.** *miR-133b* suppresses cell proliferation, migration and invasion in the EC cell lines. (A) Proliferation of the RL95 to 2 and HEC-1-A cell lines following transfection with *miR-133b* mimic or inhibitor was determined using a Cell Counting Kit-8 assay and there are significant differences at 48 and 72 h for *miR-133b* expression between mimic and NC mimic. (B) Migration of the RL95 to 2 and HEC-1-A cells lines following transfection with *miR-133b* mimic or inhibitor was investigated using a wound healing assay. Each group was observed at a magnification of x40. (C) Migration and invasion of the RL95 to 2 and HEC-1-A cell lines following transfection with *miR-133b* mimic or inhibitor was determined using transwell and matrigel assays. Each group was observed at a magnification of x40. \*  $p < 0.05$ ; \*\*  $p < 0.01$ ; \*\*\*  $p < 0.001$ ; \*\*\*\*  $p < 0.0001$ .

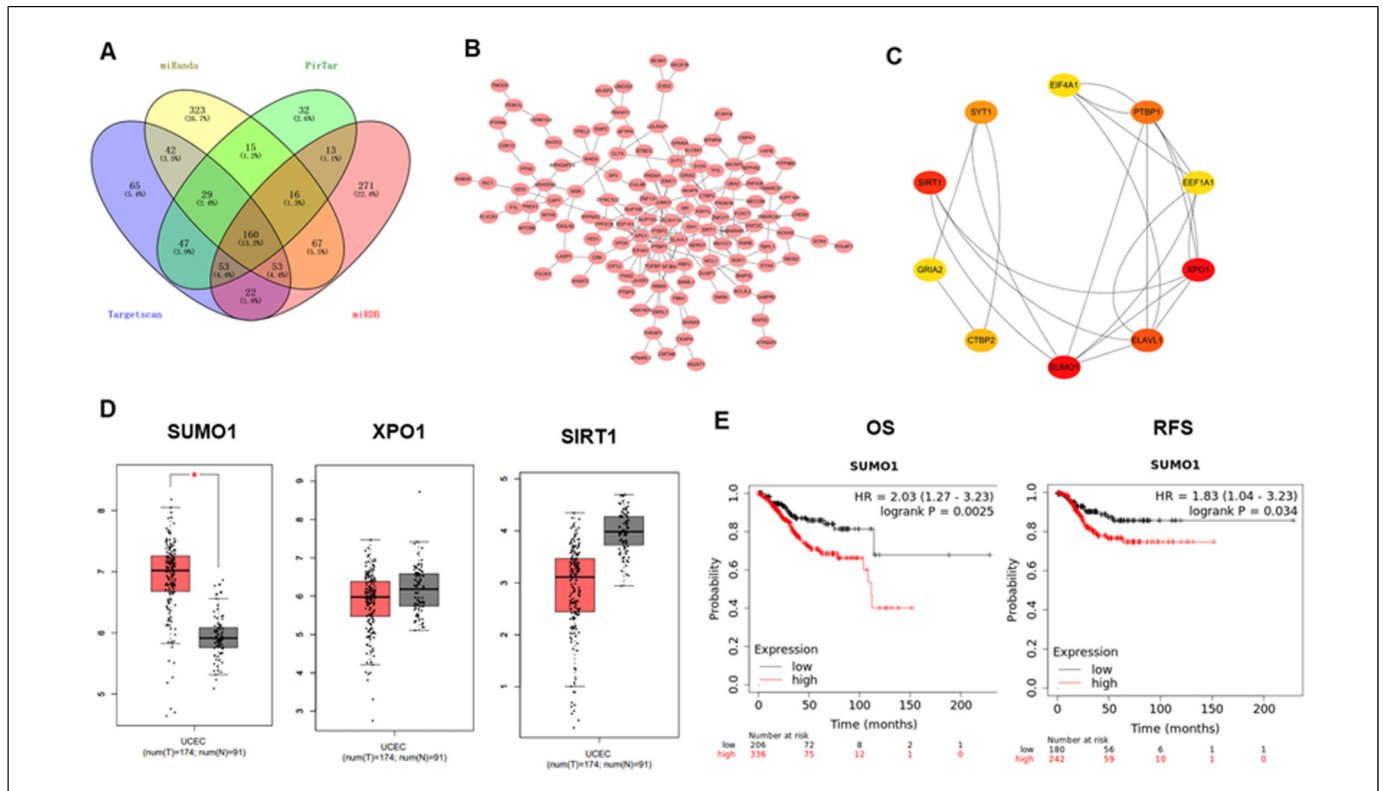


**Figure 5.** *SUMO1* is upregulated in EC and is targeted by *miR-133b*. (A) A venn diagram was used to identify the intersection of the *miR-133b* target genes predicted using the miRanda, PirTar, Targetscan and miRDB online tools. (B) A PPI network of the target genes was determined using the STRING database. (C) The Cytoscape software was used to extract hub genes from the PPI network. (D) The expression level of *SUMO1*, *XPO1* and *SIRT1* in EC and adjacent normal tissues from the GEPIA database. (E) The OS and RFS curves of *SUMO1* in EC.

### *SUMO1* Participates in *miR-133b*-Mediated Inhibition of Proliferation, Invasion and Migration in the EC Cell Lines

To further investigate whether the cellular function of *miR-133b* was mediated by *SUMO1* expression, si-*SUMO1* and *miR-133b* inhibitor were transfected into the RL95 to 2 cell lines together or separately. As shown in Figure 7A, CCK-8 analysis revealed that knockdown of *SUMO1* significantly inhibited cell viability at 24, 48 and 72 h ( $p < 0.05$ ), and the combination of *SUMO1* knockdown and *miR-133b* silencing decreased cell viability significantly at 48 and 72 h compared with that in cells transfected with *miR-133b* inhibitor ( $p < 0.01$  and  $p < 0.05$ , respectively). Similarly, the same trend was found for migration and invasion analysis in the RL95 to 2 cell line, using wound healing and transwell assays, respectively (Figure 7B and C). Subsequently, RT-q PCR and western blot assays revealed that the mRNA and protein expression levels of *SUMO1* were significantly downregulated following si-*SUMO1* transfection compared with that in the si-NC transfection group. In addition, the expression level of *SUMO1* was also markedly decreased following co-transfection with si-*SUMO1* and *miR-133b* inhibitor compared with that in cells transfected with *miR-133b* inhibitor (Figure 7D and E). These results suggested that *SUMO1* could reverse the effect of *miR-133b* using a rescue experiment. Altogether, the

results from the present study suggested that *SUMO1* was a direct downstream target of *miR-133b* and *SUMO1* interference inhibited cell proliferation, migration and invasion in the EC cell lines.

### Discussion

In the present study, it was found that *miR-133b* was downregulated in EC tissue and the low expression level of *miR-133b* was associated with positive tumor grade, tumor histology and menopause status. To identify its molecular function in EC, overexpression and knockdown experiments were used to investigate the functions of *miR-133b* in the EC cell lines. The results from the present study revealed that upregulation of *miR-133b* could inhibit the proliferation, migration and invasion of the EC cell lines. Considering that miRNAs can regulate gene expression by targeting the 3'UTR of mRNA, the miRanda, PicTar, Targetscan and miRDB online tools were used to predict the potential targets of miRNA. Using several bioinformatics tools, including Venny 2.1, STRING, Cytoscape and GEPIA, *SUMO1* was selected as the potential target gene of *miR-133b*. Then, the relationship between *miR-133b* and *SUMO1* was investigated and the results indicated that *SUMO1* could reverse the effect of *miR-133b* using rescue experiments. Thus, we hypothesized that *miR-133b* acts as an



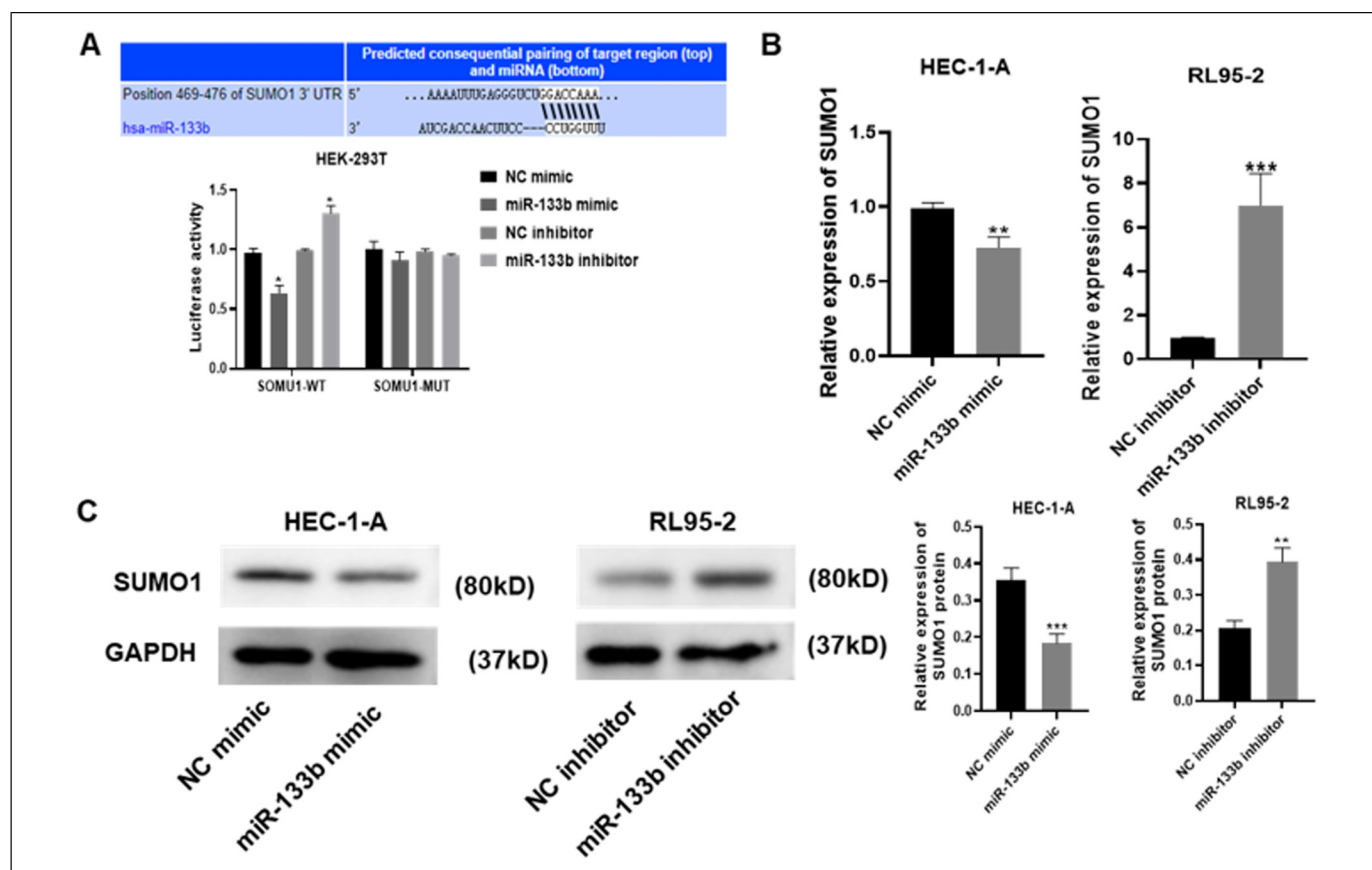


**Figure 6.** *miR-133b* downregulates the expression level of *SUMO1*. (A) Luciferase activity of *SUMO1* to 3'UTR-WT and *SUMO1* to 3'UTR-MUT in the 293 T cell lines in the presence of *miR-133b* were detected using a dual luciferase reporter assay. The significant differences indicate the differences between *SUMO1*-WT/*miR-133b* mimic and *SUMO1*-WT/NC mimic or *SUMO1*-WT/*miR-133b* inhibitor and *SUMO1*-WT/NC inhibitor. (B) Reverse transcription-quantitative PCR was used to detect the mRNA expression level of *SUMO1* in the RL95 to 2 and HEC-1-A cell lines following overexpression or knockdown of *miR-133b*. (C) A western blot assay was used to detect the protein expression level of *SUMO1* in the RL95 to 2 and HEC-1-A cell lines following overexpression or knockdown of *miR-133b*. \*  $p < 0.05$ ; \*\*  $p < 0.01$ ; \*\*\*  $p < 0.001$ ; \*\*\*\*  $p < 0.0001$ .

anti-oncogene by suppressing the expression level of *SUMO1* and *miR-133b* and *SUMO1* could be novel candidates for EC therapy.

An increasing number of studies have showed that the abnormal expression level of miRNA was associated with the occurrence and development of cancer, including EC. *miR-133b* has been proven to play different functional roles in several types of malignant tumors. For example, overexpression of *miR-133b* suppressed cisplatin resistance by targeting TUG1 in human tongue squamous cell carcinoma.<sup>25</sup> In addition, *miR-133b* was also found to be downregulated in renal cell carcinoma cell lines and weakened the cell viability, invasion and migration by targeting the ERK signaling pathway.<sup>15</sup> Furthermore, decreased *miR-133b* mRNA expression level has been reported in uterine sarcomas and in mixed epithelial-mesenchymal uterine tumors,<sup>26</sup> which was consistent with the results from the present study to a certain extent. Multivariate Cox proportional hazard model showed that low expression of *miR-126* and *miR-133b*, tumor stage and lymph node metastasis were independent prognostic factors affecting the overall survival

of patients with non small cell lung cancer.<sup>27</sup> In addition, researchers collected 154 patients with laryngeal cancer as the research subjects and 100 healthy people as the control group. The analysis results showed that the expression of *miR-133b* was significantly different from that of patients with different pathological stages and different degrees of differentiation; and receiver operating characteristic curves analysis shows that *miR-133b* has high diagnostic value for laryngeal cancer.<sup>28</sup> These results showed that *miR-133b* plays an important role in tumor and may serve as a potential target for clinical diagnosis of tumors. However, its mechanism in EC is still controversial. *SUMO1* was found to be a direct target gene, downstream of *miR-133b* and inhibition of *SUMO1* expression reduced the proliferation, invasion and migration of EC cells. *SUMO1* performs reversible post-translational modifications, that regulate nuclear transport, transcriptional regulation, apoptosis and protein stability of cells.<sup>20</sup> For example, *SUMO1* regulated tumorigenesis by modifying KHSRP to prevent the biogenesis of TL-G-RICH miRNAs.<sup>29</sup> Ginkgo biloba is a *SUMO-1* inhibitor, and could inhibit the tumorigenicity and

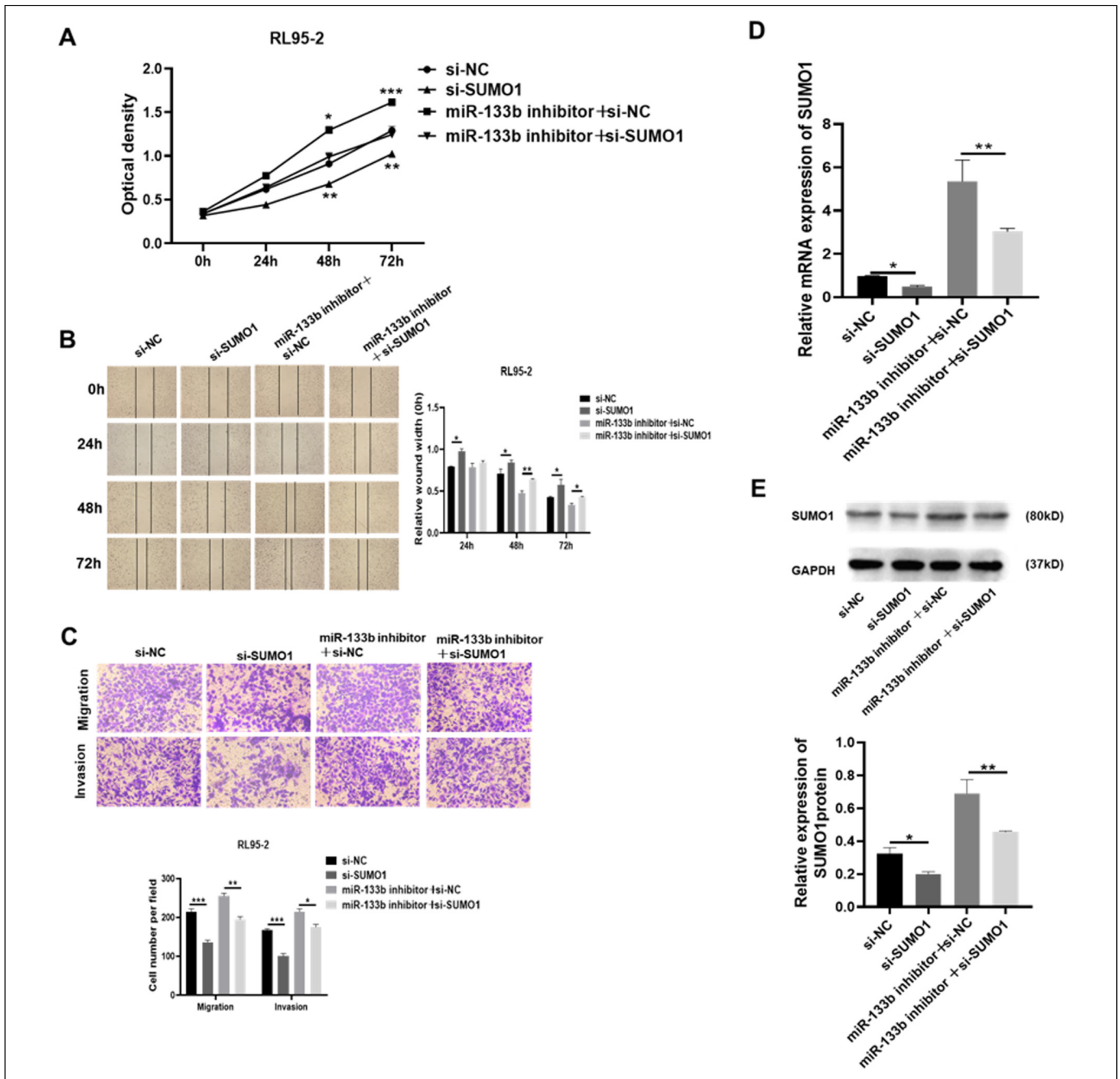


**Figure 7.** *miR-133b* affects the proliferation, invasion and migration of endometrial carcinoma cells by regulating *SUMO1*. Following inhibition of both *SUMO1* and *miR-133b* or individually in the RL95 to 2 cell line, (A) proliferation, (B) cell migration, (C) cell invasion and migration, and (D) the mRNA and (E) the protein expression levels of *SUMO1* were determined using Cell Counting Kit-8, wound healing, transwell and matrigel and assays, and RT-PCR and western blot analyses, respectively. Each group was observed at a magnification of x40. \*  $p < 0.05$ ; \*\*  $p < 0.01$ ; \*\*\*  $p < 0.001$ ; \*\*\*\*  $p < 0.0001$ .

tumor progression of oral squamous cell carcinoma by reducing the enhancement of Smad4 sumoylation induced by TGF- $\beta$ 1.<sup>30</sup> To the best of our knowledge, so far *SUMO1* has been reported in three studies investigating EC. In the first study, PGE2 promoted proliferation and invasion by enhancing the activity of *SUMO1* in EC.<sup>31</sup> In the second article, our previous study investigated the downregulation of H4 sumoylation by

silencing SUMO-1 expression; thus, inhibiting EC cell proliferation and inducing apoptosis.<sup>32</sup> In the third paper, acetylation of HIF-1  $\alpha$  protein reduced the stem maintenance ability of EC stem cells and enhanced their sensitivity to chemotherapy.<sup>33</sup> These studies suggested the potential role of *SUMO1* in EC and provided evidence to verify the results of the present study. Studies have shown that miR-423 inhibits

cisplatin-induced endometrial cancer cell apoptosis by regulating the expression of caspase3/7 and Bcl-2.<sup>34</sup> miR-199a-3p enhances the sensitivity of ovarian cancer cells to cisplatin by down-regulating the expression of ITGB8, which may become a target for the treatment of cisplatin-resistant ovarian cancer.<sup>35</sup> The above studies show that the expression of drug-resistant mRNAs and miRNAs in endometrial cancer cells treated with cisplatin or/and salinomycin is related to the difference. However, it is reported in the literature that both miR-133b and SUMO1 are not related to cisplatin/salinomycin resistance.

## Conclusion

In conclusion, the collective findings of the current study revealed that *miR-133b* was downregulated in EC tissues, and overexpression of *miR-133b* inhibited cell proliferation, migration and invasion by targeting *SUMO1*. Thus, *miR-133b* was considered to play a suppressor role in EC tumorigenesis and the *miR-133b/SUMO1* axis may be a therapeutic target for the treatment of EC. The study may provide novel insights and ideas for improving the treatment strategy of patients with EC. Despite these promising results, the limitations cannot be ignored. In our paper, there is a lack of the actual clinical evidence to verify the expression and prognosis of *miR-133b* in clinical histology. The advantage of this paper is to analyze the role of *miR-133b* in EC through bioinformatics combined with cell function tests. The shortcoming of this article is that it only conducts cell in vitro function test and has not been verified by animal in vivo experiment.

## Acknowledgements

Not applicable.

## Funding

No funding was received.

## Competing Interests

The authors declare that they have no competing interests.

## Availability of Data and Materials

Data supporting the discovery of this study are available from the corresponding authors on reasonable request.

## Authors' Contributions

LL and YC designed the experiments; JZ performed the bioinformatics analysis; XX and CT performed the experiments and analyzed the results. All authors wrote and revised the manuscript. All the authors read and approved the final manuscript. All authors agreed to be accountable for all aspects of the work in ensuring that questions related to the accuracy or integrity of any part of the work are appropriately investigated and resolved.

## Ethics Approval and Consent to Participate

Our study did not require an ethical board approval because it did not contain human or animal trials.


## Patient Consent for Publication

Not applicable.

## Competing Interests

The authors declare that they have no competing interests.

## ORCID iD

Jing Ye  <https://orcid.org/0000-0003-2347-8237>

## References

- Gao L, Nie X, Zhang W, et al. Identification of long noncoding RNA RP11-89K21.1 and RP11-357H14.17 as prognostic signature of endometrial carcinoma via integrated bioinformatics analysis. *Cancer Cell Int.* 2020;20:268.
- Morice P, Leary A, Creutzberg C, Abu-Rustum N, Darai E. Endometrial cancer. *Lancet (London, England).* 2016;387-(10023):1094-1108.
- Goad J, Ko YA, Kumar M, Jamaluddin MFB, Tanwar PS. Oestrogen fuels the growth of endometrial hyperplastic lesions initiated by overactive Wnt/ $\beta$ -catenin signalling. *Carcinogenesis.* 2018;39(9):1105-1116.
- Xu X, Zheng S. MiR-887-3p negatively regulates STARD13 and promotes pancreatic cancer progression. *Cancer Manag Res.* 2020;12:6137-6147.
- Zhang W, Ji W, Li T, Liu T, Zhao X. MiR-145 functions as a tumor suppressor in papillary thyroid cancer by inhibiting RAB5C. *Int J Med Sci.* 2020;17(13):1992-2001.
- Liu CH, Jing XN, Liu XL, Qin SY, Liu MW, Hou CH. Tumor-suppressor miRNA-27b-5p regulates the growth and metastatic behaviors of ovarian carcinoma cells by targeting CXCL1. *J Ovarian Res.* 2020;13(1):92.
- Zhang L, Ma C, Wang X, et al. MicroRNA-874-5p regulates autophagy and proliferation in pulmonary artery smooth muscle cells by targeting sirtuin 3. *Eur J Pharmacol.* 2020;888:173485.
- Correia de Sousa M, Gjorgjieva M, Dolicka D, Sobolewski C, Foti M. Deciphering miRNAs' action through miRNA editing. *Int J Mol Sci.* 2019;20(24):6249.
- Tiwari A, Mukherjee B, Dixit M. MicroRNA Key to angiogenesis regulation: miRNA biology and therapy. *Curr Cancer Drug Targets.* 2018;18(3):266-277.
- Fabian MR, Sonenberg N. The mechanics of miRNA-mediated gene silencing: a look under the hood of miRISC. *Nat Struct Mol Biol.* 2012;19(6):586-593.
- Zheng X, Xu K, Zhu L, Mao M, Zhang F, Cui L. MiR-486-5p Act as a biomarker in endometrial carcinoma: promotes cell proliferation, migration, invasion by targeting MARK1. *Oncotargets Ther.* 2020;13:4843-4853.
- Zhang HH, Li R, Li YJ, et al. eIF4E-related miR-320a and miR-340-5p inhibit endometrial carcinoma cell metastatic capability by preventing TGF- $\beta$ 1-induced epithelial-mesenchymal transition. *Oncol Rep.* 2020;43(2):447-460.

13. Du J, Zhang F, Zhang L, Jia Y, Chen H. MicroRNA-103 regulates the progression in endometrial carcinoma through ZO-1. *Int J Immunopathol Pharmacol.* 2019;33:1-8.
14. Cai X, Qu L, Yang J, et al. Exosome-transmitted microRNA-133b inhibited bladder cancer proliferation by upregulating dual-specificity protein phosphatase 1. *Cancer Med.* 2020;9-(16):6009-6019.
15. Xu Y, Ma Y, Liu XL, Gao SL. Mir-133b affects cell proliferation, invasion and chemosensitivity in renal cell carcinoma by inhibiting the ERK signaling pathway. *Mol Med Rep.* 2020;22(1):67-76.
16. Chen GY, Ruan L. Downregulation Of microRNA-133b And Its clinical value In Non-small cell lung cancer. *Onco Targets Ther.* 2019;12:9421-9434.
17. Sanyal S, Mondal P, Sen S, Sengupta Bandyopadhyay S, Das C. SUMO E3 ligase CBX4 regulates hTERT-mediated transcription of CDH1 and promotes breast cancer cell migration and invasion. *Biochem J.* 2020;477(19):3803-3818.
18. Katayama A, Ogino T, Bandoh N, et al. Overexpression of small ubiquitin-related modifier-1 and sumoylated Mdm2 in oral squamous cell carcinoma: possible involvement in tumor proliferation and prognosis. *Int J Oncol.* 2007;31(3):517-524.
19. Xu H, Wang H, Zhao W, et al. SUMO1 Modification of methyltransferase-like 3 promotes tumor progression via regulating snail mRNA homeostasis in hepatocellular carcinoma. *Theranostics.* 2020;10(13):5671-5686.
20. Zhang A, Tao W, Zhai K, et al. Protein sumoylation with SUMO1 promoted by Pin1 in glioma stem cells augments glioblastoma malignancy. *Neuro Oncol.* 2020;22(12):1809-1821.
21. Clough E, Barrett T. The gene expression omnibus database. *Methods In Molecular Biology (Clifton, NJ).* 2016;1418:93-110.
22. Martin B, Chadwick W, Yi T, et al. VENNTURE--a novel venn diagram investigational tool for multiple pharmacological dataset analysis. *PLoS One.* 2012;7(5):e36911.
23. Hou GX, Liu P, Yang J, Wen S. Mining expression and prognosis of topoisomerase isoforms in non-small-cell lung cancer by using oncomine and Kaplan-Meier plotter. *PLoS One.* 2017;12(3):e0174515.
24. Deng JL, Xu YH, Wang G. Identification of potential crucial genes and Key pathways in breast cancer using bioinformatic analysis. *Front Genet.* 2019;10:695.
25. Zhang K, Zhou H, Yan B, Cao X. TUG1/miR-133b/CXCR4 Axis regulates cisplatin resistance in human tongue squamous cell carcinoma. *Cancer Cell Int.* 2020;20:148.
26. Kowalewska M, Bakula-Zalewska E, Chechlinska M, et al. microRNAs in uterine sarcomas and mixed epithelial-mesenchymal uterine tumors: a preliminary report. *Tumour Biology : The Journal of the International Society for Oncodevelopmental Biology and Medicine.* 2013;34(4):2153-2160.
27. Chen SW, Wang TB, Tian YH, Zheng YG. Down-regulation of microRNA-126 and microRNA-133b acts as novel predictor biomarkers in progression and metastasis of non small cell lung cancer. *Int J Clin Exp Pathol.* 2015;8(11):14983-14988.
28. Zhao N, Liu H, Zhang A, Wang M. Expression levels and clinical significance of miR-203 and miR-133b in laryngeal carcinoma. *Oncol Lett.* 2020;20(5):213.
29. Yuan H, Deng R, Zhao X, et al. SUMO1 Modification of KHSRP regulates tumorigenesis by preventing the TL-G-rich miRNA biogenesis. *Mol Cancer.* 2017;16(1):157.
30. Liu K, Wang X, Li D, et al. Ginkgolic acid, a SUMO-1 inhibitor, inhibits the progression of oral squamous cell carcinoma by alleviating SUMOylation of SMAD4. *Mol Ther Oncolytics.* 2020;16:86-99.
31. Ke J, Yang Y, Che Q, et al. Prostaglandin E2 (PGE2) promotes proliferation and invasion by enhancing SUMO-1 activity via EP4 receptor in endometrial cancer. *Tumour Biology : The Journal of the International Society for Oncodevelopmental Biology and Medicine.* 2016;37(9):12203-12211.
32. Zheng J, Liu L, Wang S, Huang X. SUMO-1 Promotes ishikawa cell proliferation and apoptosis in endometrial cancer by increasing sumoylation of histone H4. *International Journal Of Gynecological Cancer : Official Journal of the International Gynecological Cancer Society.* 2015;25(8):1364-1368.
33. Yuan L, Jiang ZM, Chen XH, et al. [Hypoxia inducible factor-1 $\alpha$  deSUMOylation reduces the stemness maintenance ability of endometrial cancer stem cell and increases its chemosensitivity]. *Zhonghua yi xue za zhi.* 2017;97(45):3579-3582.
34. Li J, Sun H, Liu T, Kong J. MicroRNA-423 promotes proliferation, migration and invasion and induces chemoresistance of endometrial cancer cells. *Exp Ther Med.* 2018;16(5):4213-4224.
35. Cui Y, Wu F, Tian D, et al. miR-199a-3p enhances cisplatin sensitivity of ovarian cancer cells by targeting ITGB8. *Oncol Rep.* 2018;39(4):1649-1657.